

Precursors of order in aggregates of patchy particles

Oleg A. Vasilyev,^{1,2} Boris A. Klumov,^{3,4} and Alexei V. Tkachenko⁵

¹*Max-Planck-Institut für Intelligente Systeme, Stuttgart, Germany*

²*IV. Institut für Theoretische Physik,*

Universität Stuttgart, Stuttgart, Germany

³*Joint Institute for High Temperatures, Moscow, Russia*

⁴*Institute for Information Transmission Problems, Moscow, Russia*

⁵*Center for Functional Nanomaterials,*

Brookhaven National Laboratory, Upton, NY, USA

(Dated: December 17, 2018)

Abstract

We study computationally the local structure of aggregated systems of patchy particles. By calculating the probability distribution functions of various rotational invariants we can identify the precursors of orientation order in amorphous phase. Surprisingly, the strongest signature of local order is observed for 4-patch particles with tetrahedral symmetry, not for 6-patch particles with the cubic one. This trend is exactly opposite to their known ability to crystallize. We relate this anomaly to the observation that a generic aggregate of patchy systems has coordination number close to 4. Our results also suggest a significant correlation between rotational order in the studied liquids with the corresponding crystalline phases, making this approach potentially useful for a broader range of patchy systems.

PACS numbers: **82.70.Dd, 07.05.Tp, 61.43.Bn**

The field of colloidal and nanoparticle self-assembly has dramatically changed over the past decade due to introduction of novel classes of particles and interactions between them. This includes highly selective DNA-mediated interactions [1]-[3], use of wide variety of particle shapes and so-called "patchy" colloids [4]-[6], as well as combinations of these approaches. The patchy particles have patterns of chemically distinct regions on their surfaces that results in directional (covalent-like) interactions. This opens an appealing prospect of "programming" the symmetry of a desired structure with the symmetry of the particle. For instance, colloids with tetrahedral arrangement of patches have been widely studied theoretically [8]-[11], as a potential platform for self-assembly of diamond lattice, one of the best candidates for photonic band gap materials [7]. These studies were in part motivated by experimental demonstration of patchy colloids with tetrahedral and other symmetries [5]. Most recently, these experimental techniques evolved even further due to functionalization of patches with DNA and resulting selectivity of interactions [6].

While the equilibrium phase diagrams of such patchy colloids have been extensively studied computationally, the experimental self-assembly of crystalline morphologies will unavoidably be limited by slow kinetics. By analogy with self-assembly of colloids and nanoparticles isotropically functionalized with DNA, one might expect the system to form a random aggregate initially, and possibly be transformed to a crystal upon annealing. In this paper we focus on the relatively early stage of self assembly, and analyze the precursors of crystallinity in a (mostly) random aggregate of patchy particles. We do this by employing the set of bond order parameters [15] which have been successfully applied to a great variety of physics problems. The parameters are commonly used to determine the degree of crystallinity of a system, as well as the crystal morphology. In our case, we apply it to find traces of ordering in liquid phase, which may result in crystal formation upon annealing. This kind of analysis can potentially determine the morphology which is preferred kinetically, rather than energetically. For instance, it is well known that the space of possible structures for patchy particles with tetrahedral symmetry is highly degenerate. At least two diamond morphologies, cubic, and hexagonal have nearly the same free energy. As a result, in majorities of studies (with a rare but noteworthy exception [11]) neither of the crystals form spontaneously. In such a case, the structure in actual experiments may be selected kinetically.

Several models have been used to simulate patchy colloids. Most common are anisotropic

Lennard-Jones potential [10], and Kern-Frenkel model [12],[8],[9]. In those models, the patch geometry can be tuned independently of the interaction range, and the degree of directionality is an important parameter of the system. Since the dependence of the system behavior on the patch size is not a focus of our study, here we use a simpler model with point-like patches interacting via Gaussian potential. The range of the potential automatically determines the degree of directionality of the bond. Physically, this is a reasonable model to describe nanoparticles with locally grafted DNA molecules, in which case both patch size and range of interactions is determined by DNA gyration radius.

Numerical method Our numerical algorithm realize the description of a patchy particle as a rigid body. We represent the motion of a patchy particle of the radius R as a combination of the displacement of its center and rotation around some axis, passing through its center. We study two systems with 4 patches (4pch) and 6 patches (6pch). At the initial time moment orientation locations of four patches $\mathbf{a}_j^{(k)}(0)$, $k = 1, 2, 3, 4$ for 4pch particles with tetrahedron symmetry with respect the center of the j -th particle are $\mathbf{a}_j^{(1,2)}(0) = \left(\pm\sqrt{\frac{2}{3}}R, 0, \sqrt{\frac{1}{3}}R\right)$, $\mathbf{a}_j^{(3,4)}(0) = \left(0, \pm\sqrt{\frac{2}{3}}R, -\sqrt{\frac{1}{3}}R\right)$. For 6pch system with cubical symmetry at initial time moment patches are located at points $\mathbf{a}_j^{(1,2)}(0) = (\pm R, 0, 0)$, $\mathbf{a}_j^{(3,4)}(0) = (0, \pm R, 0)$, $\mathbf{a}_j^{(5,6)}(0) = (0, 0, \pm R)$.

The displacement of the center of the j -th particle at the time moment t is described by the vector $\mathbf{r}_j(t)$. The orientation of j -th particle at the time moment t is given by the unit quaternion $\mathbf{\Lambda}_j(t)$. That quaternion may be represented in the form (see, e.g., [13]) $\mathbf{\Lambda}_j(t) = [\cos(\phi_j(t)/2), \sin(\phi_j(t)/2)\mathbf{n}_j(t)]$, where the unit length vector $|\mathbf{n}_j(t)| = 1$ describes the axis, passing through the center of the particle and ϕ_j is the angle of rotation around this axis. We also introduce conjugated quaternion $\tilde{\mathbf{\Lambda}}_j(t) = [\cos(\phi_j(t)/2), -\sin(\phi_j(t)/2)\mathbf{n}_j(t)]$. Finally, the location of the k -th patch of the j -th particle at the time moment t is given by formula $\mathbf{a}_j^{(k)}(t) = \mathbf{r}_j(t) + \mathbf{\Lambda}_j(t) \otimes \mathbf{a}_j^{(k)}(0) \otimes \tilde{\mathbf{\Lambda}}_j(t)$ where \otimes denotes the quaternion's product. In our model cores of patchy particles repel each other with standard Lennard-Jones potential smoothly truncated at the distance $2R$ [14] with the interaction distance $\sigma = 2R$ and interaction strength $\epsilon_0 = 1$. Patches of different particles attract each other with the Gaussian potential $U_G(\mathbf{a}_{ij}^{(kl)}) = U_p \exp\left[-\left(\mathbf{a}_{ij}^{(kl)}\right)^2/2W^2\right]$, where $\mathbf{a}_{ij}^{(kl)} = \mathbf{a}_i^{(k)} - \mathbf{a}_j^{(l)}$ is a vector connecting a patch l of particle j and a patch k of particle i , $W = 0.2$ is the half-width of the interaction and U_p is the strength of the interaction. Knowing the set of all displacements and orientations of particles $\{\mathbf{r}_j, \mathbf{\Lambda}_j\}$ we can compute a set of total forces and

torques $\{\mathbf{F}_j, \mathbf{M}_j\}$ acting on every particles. We solve the following set of kinematic equations numerically using the velocity Verlet algorithm

$$\begin{cases} \dot{\mathbf{v}}_j(t) = \mathbf{F}_j(\{\mathbf{r}_j, \mathbf{\Lambda}_j\})/m \\ \dot{\omega}_j(t) = \mathbf{M}_j(\{\mathbf{r}_j, \mathbf{\Lambda}_j\})/I \end{cases}, \begin{cases} \dot{\mathbf{r}}_j(t) = \mathbf{v}_j(t) \\ \dot{\mathbf{\Lambda}}_j(t) = \frac{1}{2}\omega_j(t) \otimes \mathbf{\Lambda}_j(t) \end{cases},$$

where \mathbf{v}_j is the velocity of the j -th particle and ω_j is its angular velocity, $\dot{\mathbf{v}}_j$ and $\dot{\omega}_j$ are linear and angular accelerations, respectively. We use normalized units: the radius of particles $R = 1$, the mass is $m = 1$, the moment of inertia of a solid sphere $I = \frac{2}{5}mR^2 = 0.4$. To simulate the interaction with solvent we add Langevin terms $-\gamma\mathbf{v}_j(t) + \xi_j(t)$ and $-\frac{4}{3}\gamma R^2\omega_j(t) + \zeta_j(t)$ to forces and torques, respectively, where $\gamma = 6\pi\eta R$ is the friction coefficient for solvent viscosity η , $\xi_j(t)$ and $\zeta_j(t)$ are thermal noise terms with delta-correlated components $\langle \xi_i^\alpha(t)\xi_j^\beta(t') \rangle = 2\gamma k_B T \delta_{i,j} \delta_{\alpha,\beta} \delta_{t,t'}$, $\langle \zeta_i^\alpha(t)\zeta_j^\beta(t') \rangle = \frac{8}{3}\gamma R^2 k_B T \delta_{i,j} \delta_{\alpha,\beta} \delta_{t,t'}$. In our simulations, $k_B T = 1$ and $\gamma = 10$, therefore for times $t \gg 1/\gamma = 0.1$ the dynamics of a particle is Brownian. We simulate the system of $N = 10^3$ spherical particles of radius $R = 1$ in a cubic cell of size $L = 48$ with periodic boundary conditions. The volume fraction is $\phi = 4/3\pi R^3 N/L^3 \simeq 0.04$. We can tune the phase state of this system by varying the strength U_p of interaction potential between patches.

Structural properties To define the local structural properties of the system we use the bond order parameter method [15], which has been widely used in the context of condensed matter physics [15], hard sphere systems [16, 17], complex plasmas [18–20], colloidal suspensions [21], granular media etc. Within this method the rotational invariants of rank l of both second $q_l(i)$ and third $w_l(i)$ order are calculated for each particle i in the system from the vectors (bonds) connecting its center with the centers of its $N_{\text{nn}}(i)$ nearest neighboring particles

$$q_l(i) = \left(\frac{4\pi}{(2l+1)} \sum_{m=-l}^{m=l} |q_{lm}(i)|^2 \right)^{1/2} \quad (1)$$

$$w_l(i) = \sum_{\substack{m_1, m_2, m_3 \\ m_1+m_2+m_3=0}} \begin{bmatrix} l & l & l \\ m_1 & m_2 & m_3 \end{bmatrix} q_{lm_1}(i) q_{lm_2}(i) q_{lm_3}(i), \quad (2)$$

where $q_{lm}(i) = N_{\text{nn}}(i)^{-1} \sum_{j=1}^{N_{\text{nn}}(i)} Y_{lm}(\mathbf{r}_{ij})$, Y_{lm} are the spherical harmonics and $\mathbf{r}_{ij} = \mathbf{r}_i - \mathbf{r}_j$ are vectors connecting centers of particles i and j . We note, that the bond order parameters

$w_l \propto q_l^3$, so, in general, these parameters are much more sensitive to the local orientational order in comparison with q_l . Here, to define the structural properties of the patched particles, we calculate the rotational invariants q_l , w_l for each particle using the fixed number N_{nn} of the nearest neighbors (NN): $N_{nn} = 4, 6$ for the first shell of 4pch and 6pch systems; second shell of both systems has $N_{nn} = 12$. The first shells of the ideal 4pch and 6pch systems have cubic diamond (CD) and simple cubic (SC) lattices, respectively. The second shell has face centered cubic (FCC) lattice for both types of ideal patchy systems. We note, that formation of hexagonal diamond (HD) with hexagonal close packing (HCP) second shell is also possible for the patched system, at least kinetically.

The values of the different rotational invariants q_l and w_l for the perfect patchy crystals (for both first and second shells) are shown in Table 1. A particle whose coordinates in the 4-dimensional space (q_4 , q_6 , w_4 , w_6) are sufficiently close to those of the ideal lattice is counted as solid-like particle. By calculating the bond order parameters for the second shell it is easy to identify the disordered (liquid-like) phase as well.

TABLE I: Rotational invariants for the perfect patchy crystals

system structure		q_4	q_6	w_4	w_6
4pch	CD, HD (1st shell, 4NN)	0.509	0.628	-0.159	-0.013
6pch	SC (1st shell, 6 NN)	0.76	0.35	0.159	0.013
4,6pch	CD, SC (2nd shell, FCC)	0.191	0.575	-0.159	-0.013
4pch	HD (2nd shell, HCP)	0.097	0.485	0.134	-0.012

Figure 1 and 2 show the probability distribution functions (PDFs) of bond order parameters q_4 (a,b) and w_4 (c) at different strengths U_p of the interaction potential for the first (a) and second (b,c) shells. Figure 1 and 2 correspond to the systems with 4 and 6 patches, respectively. The MD simulations cover both uncorrelated (gas-like) and strongly coupled (liquid-like) phases. The PDFs show how the structural properties of the ensemble of patched particles vary with increase of interaction strength U_p . At low U_p (blue lines) both 4 and 6 patched systems are completely dispersed, and the PDF plots correspond to the isotropic distribution (of uncorrelated system). Increase of U_p results in formation of aggregates of patchy particles; in the final state, nearly all particles consolidate into a few big clusters.

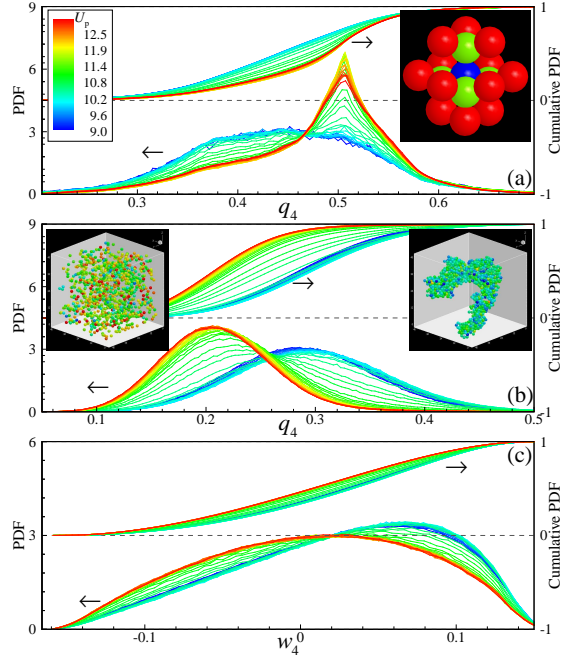


FIG. 1: (Color online) Patchy system 4pch. Probability distribution functions (PDFs) versus q_4 (a,b) and w_4 (c) at different strengths U_p of the interaction potential for the first (a) and second (b,c) shells. Cumulative distributions of the PDFs are also plotted to quantify the liquid-solid transition in the system. The curves are color-coded by U_p value. Inset (a) shows first (green) and second (red color) shells of the perfect crystalline particle. Insets (b) show initial gaseous (b, left) and final gel-like (b, right) particle distribution over space. Particles are color-coded by q_6 value.

Review of the plots for the first shell reveal a remarkable and counterintuitive result. There is a strong evidence of local tetrahedral ordering for 4pch particles, represented by a spike at $q_4 = 0.5$, but very weak order for particles with cubic symmetry. This goes exactly contrary to the known crystallization properties of these systems: as we have discussed earlier, 4pch particles are notoriously hard to crystallize, as opposed to 6pch. The second shell PDF of q_4 shows a pronounced but wide peak centered around $q_4 = 0.2$, which is very close to the value expected for ideal FCC lattice. Note that the second shell of both SC and CD lattices has FCC symmetry. It is therefore possible that this peak is a precursor

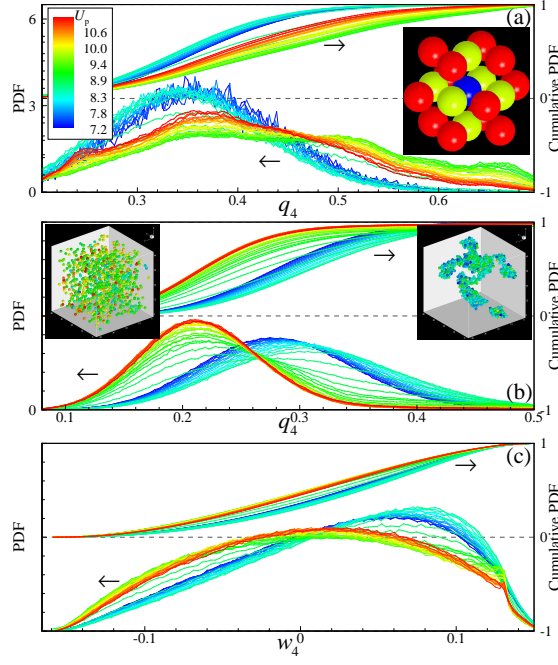


FIG. 2: (Color online). Patchy system 6pch. Probability distribution functions (PDFs) versus q_4 (a,b) and w_4 (c) at different strengths U_p of the interaction potential for the first (a) and second (b,c) shells. Cumulative distributions of the PDFs are also plotted to quantify the liquid-solid transition in the system. The curves are color-coded by U_p value. Inset (a) shows first (green) and second (red color) shells of the perfect crystalline particle. Insets (b) show initial gaseous (b, left) and final gel-like (b, right) particle distribution over space. Particles are color-coded by q_6 value.

of the future crystalline order. In order to confirm this correlation, additional studies of a broader class of systems will be needed. If that is the case, it will imply that 4pch system prefers CD structure over HD, at least kinetically. Note that w_4 does not show any clear signature of FCC order, but that may be due to the fact that it is a higher-order invariant than q_4 . In general both q_4 and w_4 PDFs look remarkably similar for both systems, which may originate from the similarity between the second shell structure of SC and CD, but may also be a generic property of amorphous aggregates of patchy particles. It noteworthy that 6pch exhibits very sharp but weak peak at $w_4 \approx 0.13$. This value is close to the one for HCP

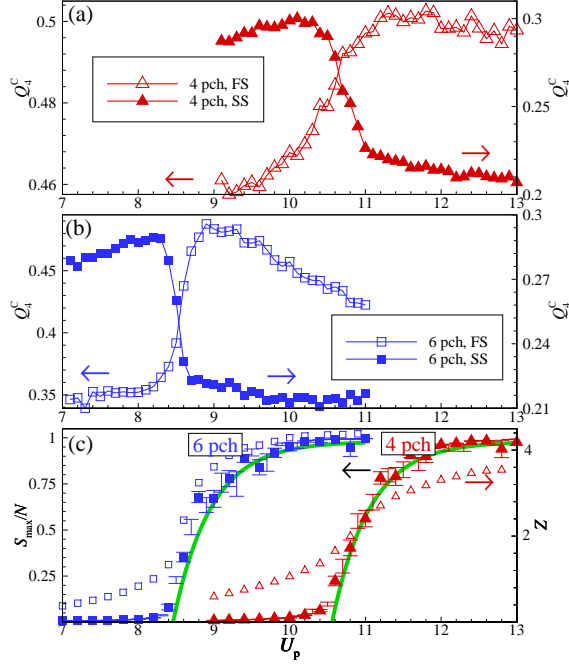


FIG. 3: (Color online) (a), (b) The order parameters, characterizing the crystallization of the system with 4pch (a,c) and 6pch patches (b,c) and associated with the cumulative PDFs versus q_4 value are plotted as a function of the particle interaction potential strength U_p for both first (FS, open triangles and squares) and second (SS, filled triangles and squares) shells. Panel (c) shows the normalized maximal cluster size S_{\max}/N (solid squares and triangles) and average coordination number Z (open squares and triangles) as functions of U_p . Solid green lines correspond to analytical fitting discussed in text.

order, but its actual origin is unclear at the moment. The HCP order is inconsistent with the cubic arrangement of the patches, and w_4 value alone does not allow for an unambiguous interpretation.

The cumulative distributions $C_q(q_4)$ and $C_w(w_4)$ are also presented in Figures 1 and 2. One can use the half-height positions for these curves as order parameters that characterize the local orientational order. For instance, Q_4^C is defined based on cumulative distribution of $C_q(q_4)$ as $\int_{-\infty}^{Q_4^C} C_q(q_4) dq_4 \equiv 1/2$. Its value for both first and second shells are plotted in

Figure 3 as a function of U_p for both patchy systems. Note that the completely isotropic distribution corresponds to non-zero values of Q_4^C due to a finite number of particles in each shell. The deviation from that values characterizes the degree of orientational correlations in the system. We observe a clear crossover from isotropic gas phase to strongly correlated liquid at high values of U_p .

In order to understand the reason for the striking difference in the first-shell orientational order between the two systems, we will now consider their topological properties. Two patches are defined to be bound if they are closer than $2W$ from each other (where $W = 0.2$ is the width parameter of the Gaussian potential). This allows us to construct clusters of connected particles and compute the fraction of particles that belong to the maximum cluster, S_{\max}/N . In addition, we determine the mean coordination number Z , i.e. the average number of neighbors to which a particle is connected. Both properties are presented in Figure 3 together with cumulative bond orientation parameter Q_4^C discussed above. Naturally, the signature of aggregation appears simultaneously on all the plots. Remarkably, the coordination number in both systems exhibits saturation at value $Z \approx 4$, despite the particle having dramatically different design and number of patches. This observation is the key to understanding the difference in first shell ordering. Indeed, this value of Z means that 4pch particles in random aggregate have almost the same number of bonds as in ideal diamond crystal, either cubic or hexagonal. Hence, the first shell exhibits strong tetrahedral ordering. On the other hand, at $Z = 4$ the 6pch system is far from connectivity of the corresponding simple cubic lattice, and the orientational order is far less pronounced.

The dependence of the largest cluster size on U_p can be also related to the value of Z . The concentration of free particles depends exponentially on the chemical potential of those belonging to the aggregate, $\mu = ZU_p/2 + \text{const}$. The size of the biggest cluster can be therefore estimated by subtracting the gas-like fraction of the system from the total: $S_{\max}/N = 1 - \exp(-Z(U_p - U_0)/2)$. This formula with $Z=4$ well describes the numerical results, as shown in Fig. 3(c). The relative shift of the two plots can be attributed to an additional entropy of the 6pch liquid. This entropy, $\Delta S \approx 4k_B$ per particle reflects a much larger number of ways in which 6-patch system can be arranged into $Z = 4$ network.

What determines the coordination number of the amorphous aggregate? In the limit of infinitely short range of interactions between patches, and hard-core interparticle repulsion, the bond orientation and relative positions of the two bound particles would be completely

restricted. The only remaining degree of freedom would be rotation about the direction of the bond. This means that each perfect bond freezes 5 translational and orientational degrees of freedom (or $2d - 1$ in d dimensions). Since the total number of degrees of freedom for N particles is $d(d + 1)N/2$, the system becomes completely rigid and incapable of creating new bonds for coordination number $Z_{\text{rigid}} = d(d + 1)/(2d - 1) = 2.4$ for $d = 3$. This result represents conceptually important but somewhat unrealistic case from both experimental and computational points of view. Both interactions between patches and interparticle repulsions have finite range which means that bonds are not infinitely rigid. Interestingly, out of 5 degrees of freedom that a perfectly rigid bond would suppress, not all are equally affected in the case of finite interaction range. If λ_1 is the typical range of intra-patch attraction, and λ_2 is that of interparticle repulsion, a single bond results in an angular confinement of a particle within solid angle $\delta\Omega \simeq 4\pi(\lambda_1 + \lambda_2)/R$. This means that each of the angular coordinates is constrained much weaker in relative terms, than the translational degrees of freedom of the bound patches, $\delta\theta \simeq \sqrt{\frac{(\lambda_1 + \lambda_2)}{R}} \gg \frac{\lambda_1}{R}$. If we now repeat the above counting argument by only assuming each bond to suppress d translational degrees of freedom, we obtain a new estimate of the coordination number of the amorphous aggregate $Z^* = d + 1 = 4$ for $d = 3$. This value of Z is indeed consistent with our results, and also plays a prominent role in a other important problems. For instance, it corresponds to isostatic packing of objects with infinite friction coefficient.

To summarize, the random aggregation naturally results in a liquid with coordination number close to $Z^* = 4$. This is close to maximum connectivity of 4pch particles, but is substantially below that for 6pch system. As a result, the bond orientational order is much more pronounced in the first shell of particles with tetrahedral symmetry than for those with cubic ones. Paradoxically, this also means much lower driving force towards crystallization in the tetrahedral case. This complements the well known problem of degeneracy of the ground state of the system: not only is there a competition between energetically very similar cubic and hexagonal diamond, but both of them have very little advantage in connectivity over generic aggregate with $Z \approx Z^* = 4$. The 6pch system on the other hand has a clear energetic incentive to form a well coordinated SC crystal. Altogether this explains both why the diamond is so hard to self-assemble and also the anomalous orientational order that we report for 4pch liquid. In addition, our analysis of the second shell organization reveal signatures consistent with FCC ordering in both system, which is indeed expected in the corresponding

crystals, SC for 6pch and CD for 4pch. The use of RI-based analysis developed in this work on a broader range of patchy systems will be a useful tool to characterize seemingly structureless aggregates, and capture early precursors of order.

Research is supported by European Research Council under FP7 IRSES Marie-Curie grants PIRSES-GA-2010-269139 and PIRSES-GA-2010-269181. BAK was supported partially by the Russian Foundation for Basic Research, Project no. 13-02-00913. Research carried out in part at the Center for Functional Nanomaterials, Brookhaven National Laboratory, which is supported by the U.S. Department of Energy, Office of Basic Energy Sciences, under Contract No. DE-AC02-98CH10886.

-
- [1] C. A. Mirkin, R. L. Letsinger, R. C. Mucic, & J.J. Storhoff, *Nature* **382**, 607–609 (1996).
 - [2] D. Nykypanchuk, M. M. Maye, D. van der Lelie, & O. Gang, *Nature* **451**, 549–552 (2008).
 - [3] S. Y. Park et al. *Nature* **451**, 553–556 (2008).
 - [4] S. C. Glotzer, & M. J. Solomon, *Nature Mater.* **6**, 557–562 (2007).
 - [5] V. N. Manoharan, M. T. Elsesser, & D. J. Pine, *Science* **301**, 483–487 (2003).
 - [6] Y. Wang et al. *Nature* **491**, 51–55 (2012).
 - [7] M. Maldovan and E. L. Thomas, *Nature Mater.* **3**, 593 (2004).
 - [8] F. Romano, E. Sanz & F. Sciortino, *J. Chem. Phys.* **134**, 174502–174508 (2011).
 - [9] F. Romano, E. Sanz, and F. Sciortino, *J. Phys. Chem. B* **113**, 15133 (2009).
 - [10] E. G. Noya, C. Vega, J. P. K. Doye, and A. A. Louis, *J. Chem. Phys.* **132**, 234511 (2010).
 - [11] Z. Zhang, A. S. Keys, T. Chen, and S. C. Glotzer, *Langmuir* **21**, 11547 (2005).
 - [12] N. Kern and D. Frenkel, *J. Chem. Phys.* **118**, 9882 (2003).
 - [13] C. F. F. Karney, *J. Mol. Graph. Mod.*, **25**, 595 (2007).
 - [14] S. K. Das et al, *J. Chem. Phys.* **125**, 024506 (2006).
 - [15] P. Steinhardt et al., *Phys. Rev. B.*, **28**, 784 (1983).
 - [16] I. Volkov, M. Cieplak, J. Koplik et al, *Phys. Rev. E*, **66**, 061401 (2002).
 - [17] B. A. Klumov, S. A. Khrapak, and G. E. Morfill, *Phys. Rev. B* **83**, 184105 (2011).
 - [18] M. Rubin-Zuzic et al, *Nature Phys.* **2**, 181 (2006).
 - [19] B.A. Klumov, *Phys. Usp.*, **53**, 1053 (2010).
 - [20] S. A. Khrapak, B.A. Klumov, P. Huber et al, *Phys. Rev. Lett.*, **106**, 205001 (2011).

[21] U. Gasser, E. R. Weeks, A. Schofield et al, Science, **292**, 5515, (2001).